MOLECULAR AND CELLULAR BIOLOGY, Jan. 2004, p. 796–808 Vol. 24, No. 2
0270-7306/04/$08.00+0 DOI: 10.1128/MCB.24.2.796–808.2004

Targeted Expression of the Class II Phosphoinositide 3-Kinase in *Drosophila melanogaster* Reveals Lipid Kinase-Dependent Effects on Patterning and Interactions with Receptor Signaling Pathways

Lindsay K. MacDougall,[1]* Mary Elizabeth Gagou,[1] Sally J. Leevers,[2] Ernst Hafen,[3] and Michael D. Waterfield[4,5]

Biomolecular Sciences, University of Manchester Institute of Science and Technology, Manchester M60 1QD,[1] Cancer Research UK, London WC2 3PX,[2] Ludwig Institute for Cancer Research, Royal Free and University College Medical School, London W1W 7BS,[4] and Department of Biochemistry and Molecular Biology, University College London, London WC1E 6BT,[5] United Kingdom, and Zoologisches Institut, Universität Zürich, CH-8057 Zürich, Switzerland[3]

Received 18 July 2003/Accepted 13 October 2003

Phosphoinositide 3-kinases (PI3Ks) can be divided into three distinct classes (I, II, and III) on the basis of their domain structures and the lipid signals that they generate. Functions have been assigned to the class I and class III enzymes but have not been established for the class II PI3Ks. We have obtained the first evidence for a biological function for a class II PI3K by expressing this enzyme during *Drosophila melanogaster* development and by using deficiencies that remove the endogenous gene. Wild-type and catalytically inactive PI3K_68D transgenes have opposite effects on the number of sensory bristles and on wing venation phenotypes induced by modified epidermal growth factor (EGF) receptor signaling. These results indicate that the endogenous PI3K_68D may act antagonistically to the EGF receptor-stimulated Ras–mitogen-activated protein kinase pathway and downstream of, or parallel to, the Notch receptor. A class II polyproline motif in PI3K_68D can bind the Drk adaptor protein in vitro, primarily via the N-terminal SH3 domain of Drk. Drk may thus be important for the localization of PI3K_68D, allowing it to modify signaling pathways downstream of cell surface receptors. The phenotypes obtained are markedly distinct from those generated by expression of the *Drosophila* class I PI3K, which affects growth but not pattern formation.

Phosphoinositide 3-kinases (PI3Ks) signal to activate downstream molecules through the generation, within cellular membranes, of specific lipids that are phosphorylated at the D-3 position of the inositol ring. These lipids function as second messengers and appear to be involved in processes such as mitogenesis, cell survival, growth, differentiation, adhesion, motility, and vesicle trafficking (reviewed in reference 67). Hence, PI3Ks have been the focus of intensive research. In multicellular organisms, PI3Ks occur as a family of enzymes (40, 67). These can be assigned to three separate classes (class I, class II, and class III) based on their domain structures, differences in catalytic activity towards defined substrates, and modes of regulation. For many of the downstream events mediated by PI3K activation, the exact nature of the PI3K involved has not been defined.

The class I PI3Ks are heterodimers that associate with cell surface receptors via an adaptor subunit (reviewed in reference 67). Two class I PI3K subclasses have been identified. The prototypical class I_A PI3Ks are composed of a catalytic p110 subunit and a regulatory subunit. The regulatory subunit contains two SH2 domains that bind phosphotyrosine residues in specific motifs on activated tyrosine kinase receptors or receptor substrates; this interaction results in translocation of the associated catalytic activity to its lipid substrates at the membrane. A number of distinct adaptor subunits (50 to 85 kDa) and p110 subunits (p110α, p110β, and p110δ) have been identified. These show some variation in tissue distribution. The use of isoform-specific inhibitory antibodies has identified distinct roles for different p110 isoforms in regulating cell motility and cytoskeletal changes or in mitogenesis, but these are dependent on both receptor and cell type (reviewed in reference 67). PI3Kγ represents a separate subclass of PI3Ks (class I_B) that is activated by Gβγ subunits via a distinct p101 regulatory subunit (63).

The third class of PI3Ks are homologues of Vps34. The *VPS34* gene was originally identified through studies of mutants defective in sorting proteins to the yeast vacuole, indicating an involvement of this PI3K in protein trafficking (28). Vps34 also appears to act in an osmotic stress-activated pathway (22). TheVps34 catalytic subunit associates with a protein kinase, Vps15, which appears to constitutively localize Vps34 to the Golgi membrane and may play a role in activation of the lipid kinase. Like the class I heterodimers, the Vps34-Vps15 holoenzyme forms an evolutionarily conserved complex of regulatory and catalytic subunits responsible for its distinct subcellular localization and substrate specificity. Analogous sorting mechanisms exist in higher eukaryotes, and homologues of Vps34 have been identified in a range of multicellular organisms, including humans (69) and flies (39).

Class II PI3Ks were originally identified by sequence homology with other PI3Ks (40). In *Drosophila melanogaster* (PI3K_68D) (40, 44) and *Caenorhabditis elegans* (CE05832, encoded by the F39B1.1 gene), a single species is present, while in mammals three forms have been identified, i.e., PI3K-C2α (also termed mcpk and p170) (20, 44, 68), PI3K-C2β (2, 11),

* Corresponding author. Mailing address: Biomolecular Sciences, UMIST, P.O. Box 88, Manchester M60 1QD, United Kingdom. Phone: 44 161 200 4222. Fax: 44 161 236 0409. E-mail: lindsay.macdougall@umist.ac.uk.

and PI3K-C2γ (43, 47). PI3K-C2α and PI3K-C2β show an essentially ubiquitous distribution, while the expression of PI3K-C2γ is restricted, principally to the liver. These proteins have a modular core comprising four PI3K homology regions: HR4, a Ras binding domain analogous to those in Raf and RalGDS that is a member of the ubiquitin-like structural superfamily; HR3, a C2 domain; HR2, a helical domain that is a member of the ARM repeat structural superfamily; and HR1, a catalytic domain (40; Flybase report for *Pi3K68D*/CG11621, http://fly.ebi.ac.uk:7081/.bin/fbidq.html?FBgn0015278). In contrast to class I PI3Ks, a Ras-binding function has not been demonstrated for a class II PI3K (2). Class II PI3Ks are larger than other PI3Ks (PI3K_68D is 210 kDa) due to extensions at both the amino and carboxy termini. The C terminus contains a PX (NADPH oxidase homology) domain (48) and a further, characteristic, C2 domain. Within the N-terminal region some, but not all, class II members also contain one or more polyproline motifs which may mediate interactions with SH3 or WW domains. The functions of the class II-specific sequences are unclear. In some molecules, C2 domains mediate interactions that are regulated by calcium ions (58). Both C2 domains in class II PI3Ks, however, lack the critical aspartate residues that form the calcium binding pocket (40). Thus, analysis of the primary sequence has provided few clues as to the function and regulation of this class of enzymes. In particular, a regulatory subunit has not been identified, and little is known about how these PI3Ks are activated or the biological processes that they control.

Studies on class II PI3Ks in mammalian cells have focused on signaling pathways which have been shown, using inhibitors, to involve a PI3K; some of these do not seem to be mediated by the known class I enzymes. Thus, PI3K-C2α has been reported to lie downstream of the monocyte chemotactic peptide-1 chemokine receptor (66), the insulin receptor (12), and the epidermal growth factor (EGF) receptor (EGFR) (3). PI3K-C2β can be activated following stimulation of the integrin $\alpha_{IIb}\beta_3$ with fibrinogen (74) and has been reported to be a target of the activated receptors for EGF and platelet-derived growth factor (3) and to associate with the stem cell factor receptor, c-kit (4). In each of these cases the biological process involved appears to require signaling by both class I and class II PI3Ks.

The three classes of PI3Ks differ in substrate specificity. In vitro, class I PI3Ks have a broad substrate specificity, phosphorylating the phosphoinositides (PIs) PI, PI4P, and $PI(4,5)P_2$ at the D-3 position. In vivo, however, the major lipid signal generated by the class I enzymes is believed to be $PI(3,4,5)P_3$, which can interact with specific pleckstrin homology domains in target proteins such as phosphoinositide-dependent kinase 1 and protein kinase B. These protein kinases appear to mediate many of the processes in which class I_A PI3Ks have been implicated (reviewed in reference 67). In contrast, class III enzymes only phosphorylate PI to generate PI3P, consistent with a short activation loop which may be insufficient to accommodate the more highly phosphorylated PI substrates (70). PI3P can interact with FYVE fingers. This motif is commonly found in proteins which function at endosomes (reviewed in reference 67). The class II enzymes lack the critical lysine residue which, in class I enzymes, contacts the 5′ phosphate of $PI(4,5)P_2$ (70); hence, they can generate PI3P and $PI(3,4)P_2$ in vitro, but neither the signal generated in vivo nor its protein targets have been defined. Each of the three classes of PI3K can thus generate a different spectrum of 3-phosphorylated lipids, clearly providing the potential to signal to distinct targets.

Functional analyses of PI3Ks have been complicated by the presence of multiple members of each class in mammalian cells. In contrast, *Drosophila* has only one member of each of the three classes (40). These are named after their chromosomal location: class I is Dp110/*PI3K_92E*, class II is *PI3K_68D*, and class III is DVps34/*PI3K_59F*. Analysis of the function of each *Drosophila* PI3K may, therefore, indicate the prototypical function of each class of enzyme. Of particular interest are the class I and class II PI3Ks, since these are restricted to multicellular organisms and may thus participate in signaling between cells.

As an unbiased method of identifying cellular processes involving class II PI3K signaling, we have looked at the effects of expressing *PI3K_68D* within *Drosophila* imaginal disks. These are sheets of epithelial cells that are set aside within the embryo and which proliferate, grow, and pattern during larval life. Reorganization of these cells during metamorphosis generates the adult cuticular structures, such as the wings and eyes (16). Many of these structures are not essential for viability under laboratory conditions, and hence severe developmental defects can still be studied. *Drosophila* thus represents an ideal system in which to generate phenotypes by targeted expression. In this study we have used both wild-type and catalytically inactive versions of PI3K_68D in order to identify effects that are dependent on the lipid signal. We found that ectopic expression of wild-type and mutated versions of *PI3K_68D* in the larval imaginal disks affected the development of the wing veins, the wing margin, and the number of external sense organs. These results suggested a role for this PI3K in signaling pathways affecting patterning, and we describe genetic interactions with the EGF receptor and Notch pathways. In contrast, class I PI3Ks affect growth but not patterning (37). These results provide the first evidence for different roles for class I and class II PI3Ks in vivo and indicate that the lipid signals produced by these separate classes have distinct biological targets.

MATERIALS AND METHODS

Fly stocks. Gal4 was expressed ubiquitously under the control of the heat shock promoter; in the wing pouch (especially the dorsal region) by using Gal4-MS1096 (13), an insertion in the *Beadex* gene (42); in a stripe along the A/P boundary and at lower levels in the A compartment by using Gal4-*ptc* (559.1) (29); and in epidermal cells by using Gal4-69B (9). UAS-*Dp110* (37) and UAS-tor^{4021}-*EGFR* (21) have been described previously. UAS-*aos* (54) was kindly provided by Mandy Simcox. An activated form of the EGFR ($EGFR^{ElpE1}$) hypomorphic (drk^{10626}) (60) and antimorphic (drk^{e0A}) (59) alleles of *drk*, the loss-of-function mutations in *Notch* ($N^{264\text{-}39}$ and *notchoid*), and the deficiencies *Df*(*3L*)*vin2*, *Df*(*3L*)*vin3*, *Df*(*3L*)*vin4*, *Df*(*3L*)*vin6*, and *Df*(*3L*)*vin7* (1, 17) were obtained from Kathy Matthews at the Bloomington Stock Center. *Df*(*3L*)*vin66* was provided by Christian Lehner. $Dp110^A$, a deletion of the *PI3K_92E* gene, has been described previously (72).

Plasmid constructs. Constructs were verified by their restriction sites and by sequence analysis with an Applied Biosystems 373A automated DNA sequencer. All PCR-amplified sequences were confirmed by sequencing. Sequences of the oligonucleotides used for PCR and site-directed mutagenesis are available upon request from the corresponding author.

PI3K_68D constructs. All numbering of amino acids or nucleotides is from the initiating methionine (M_1) or ATG (A_1TG) in the *PI3K_68D* cDNA.

Plasmids carrying *PI3K_68D* (WT-*PI3K_68D*) and a catalytically inactive variant (KD-*PI3K_68D*) were generated in the pUAST vector, in which cDNAs are expressed under the control of five Gal4 binding sites (9). An N-terminal tag for the c-*myc* epitope (EQKLISEEDL) was incorporated. This is recognized by the monoclonal antibody 9E10 (23). The tag was introduced by using the *BamH1* cassette in pSK (pSK-68D) (40) as a template. The *myc*-tagged cassette (pSKmyc68D) was then digested with *Bam*HI and inserted into the *Bgl*II site of pUAST.

To generate the catalytically inactive *PI3K_68D* construct, Asp_{1457} (GAC) within the kinase domain was mutated to Ala ($GC_{4370}C$) by using pSKmyc68D as a template and the Chameleon double-stranded site-directed mutagenesis kit (Stratagene). The *Eco*RV site (GATATC) was also altered ($GT_{3354}TATC$) to facilitate selection of the mutated plasmid. The *Bam*HI cassette incorporating the mutation was then inserted into the *Bgl*II site of pUAST. The same approach was used to introduce mutations ($P_{407}A$, $P_{410}A$, and $R_{412}Q$) in the polyproline motif PPPLPPR to generate pSKmyc68D^{PII}.

An *Eco*RI cassette incorporating the wild-type sequence was also generated by the PCR overlap extension method (30). Primers were used to mutate the two internal *Eco*RI sites ($A_{4956}G$ and $A_{4965}G$) and to introduce an *Eco*RI site 3′ to both the stop codon and 3′ *Bam*HI site. A 1.4-kb fragment incorporating these changes was amplified, digested with *Xho*I and *Asp*718, and exchanged for the *Xho-Asp*718 fragment in *myc*-tagged pUAST *PI3K_68D*.

To generate an amino-terminal fragment of *PI3K_68D* (N-PI3K_68D) containing the polyproline motifs **R_{123}**MQP**t**N**P_{129}** and P_{455}**P**PL**P**P**R_{461}**, a 1,446-bp fragment corresponding to the first 470 amino acids of *PI3K_68D* was amplified from the WT-*PI3K_68D* construct (described above). A 5′ *Nde*I site and a 3′ *Xho*I site were introduced. The fragment was digested with these restriction enzymes and inserted into the same sites in the pET-16α His tag expression vector (Novagen). An amino-terminal fragment, N^{PII}-PI3K_68D, containing mutations in the second polyproline motif PII ($P_{407}A$, $P_{410}A$, and $R_{412}Q$) was generated in the same manner but with pSKmyc68D^{PII} as a template. Mutations in the first polyproline motif, PI ($R_{123}Q$, $P_{126}A$, and $P_{129}A$) were introduced in the N-PI3K_68D fragment by using the PCR overlap extension method to generate N^{PI}-PI3K_68D. A further construct incorporating mutations in both polyproline motifs, N$^{PI;\ PII}$-PI3K_68D, was generated by using the PCR overlap extension method with the singly mutated templates.

Generation of recombinant GST-SH3 fusion proteins. The glutathione *S*-transferase (GST)–Drk, GST-Drk^{W36A}, and GST-Drk^{W189A} constructs were generously provided by Tony Pawson (46, 50). The GST-Drk$^{W36A;W189A}$ plasmid was produced by the double ligation of a 304-bp *Bam*HI-*Bgl*I fragment (from the plasmid for GST-drk^{W36A}) and a 331-bp *Bgl*I-*Eco*RI fragment (from the plasmid κencoding GST-Drk^{W189A}) into the $pGEX_{KT}$ vector (Pharmacia) digested with *Bam*HI and *Eco*RI. Plasmids encoding GST fusion proteins for the individual SH3 domains of Drk (N-terminal SH3, amino acids 1 to 72; C-terminal SH3, amino acids 154 to 211) were generated by PCR amplification with the GST-Drk construct as a template. The amplified fragments were digested with *Bam*HI and *Eco*RI and inserted into the same sites in the $pGEX_{KT}$ vector.

The GST-p120 RasGAP SH3 domain was generated by Simon Woodcock from p120 RasGAP (24) and provided by David Hughes.

Plasmids encoding GST fusion proteins for the individual SH3 domains of *Src64B* (SwissProt accession number P00528; amino acids 96 to 158); *Ab*l (SwissProt accession number P00522; amino acids 196 to 270); *DPLC*γ/small wing (sl) (Protein Identification Resource accession number A53970; amino acids 824 to 890); α-spectrin (SwissProt accession number P13395; amino acids 970 to 1043), and β_H-spectrin/karst (kst) (Protein Identification Resource accession number A37792; amino acids 835 to 916) were generated by PCR amplification. First-strand cDNA, prepared from *Drosophila* poly(A)$^+$ RNA as described previously (40), was used as a template. Restriction sites were incorporated at the 5′ (*Eco*RI) and 3′ (*Xho*I) ends to facilitate subcloning into these sites in the $pGEX_{KG}$ vector (26).

Southern hybridizations. Genomic DNA was digested with *Xho*I, fractionated on 0.8% agarose gels, and transferred to Hybond N$^+$ (Amersham). Probes corresponding to the 5′ and 3′ ends of the *PI3K_68D* coding sequence (nucleotides −26 to +1063 and + 5116 to +5979, respectively, numbered relative to the coding sequence) were generated by PCR and labeled to the same specific radioactivity with [γ-^{32}P]dCTP by using a Multiprime kit (Amersham). Radioactive bands (5.7-kb 5′ fragment and ~4.5-kb 3′ fragment) were detected and quantified with a PhosphorImager (Molecular Dynamics). Since the deficiency stocks are heterozygous, those which deleted the *PI3K_68D* gene gave a signal with half the intensity of an *Oregon R* control. Values were normalized between samples by using a probe for the Dp110 gene, *PI3K_92E*, which maps to a separate region of the *Drosophila* chromosome.

Generation of transformants. Transgenic flies were generated by injecting Qiagen-purified plasmid DNA into *yw* embryos and selected on the basis of expression of the mini-white gene (7). For upstream activating sequence (UAS) constructs, several independent lines were generated for each plasmid to rule out insertion-specific effects. We found that different insertions for the same construct induced similar phenotypes with different degrees of severity.

Biochemical analyses. (i) Expression of transgenes. Heat shock Gal4-induced expression of UAS transgenes was achieved by incubating adult flies at 37°C for 1 h and then at 25°C for 4 to 6 h. Flies were lysed in 20 mM HEPES (pH 7.5)–150 mM NaCl–2 mM EGTA–1.5 mM $MgCl_2$–10% (vol/vol) glycerol containing 1% (wt/vol) Triton X-100, 0.1% β-mercaptoethanol, 5 mM benzamidine, 0.2 mM phenylmethylsulfonyl fluoride, and 100 mU of aprotinin (Sigma) ml^{-1}. To maintain the phosphorylation state of the *Drosophila* EGFR (DER), the protein phosphatase inhibitors sodium orthovanadate (1 mM), β-glycerophosphate (10 mM), molybdate (1 mM), tetrasodium pyrophosphate (1 mM), and sodium fluoride (10 mM) were included. Lysates were clarified by centrifugation.

(ii) Expression of recombinant fusion proteins in bacteria. *Escherichia coli* DH5α cells containing plasmids encoding the GST fusion proteins were grown to an optical density at 600 nm of 0.6. Expression of the fusion proteins was induced at 27°C with 0.4 mM IPTG (isopropyl-β-D-thiogalactopyranoside) for 4 h. Bacterial pellets were sonicated in phosphate-buffered saline lysis buffer (140 mM NaCl, 2.7 mM KCl, 10 mM Na_2HPO_4, 1.8 mM KH_2PO_4 [pH 7.3]) containing 1% Triton X-100, 2 mM EDTA, 5 mM benzamidine, 0.2 mM phenylmethylsulfonyl fluoride, and 0.1% mercaptoethanol and clarified by centrifugation. The extract was incubated with glutathione-agarose (Pharmacia) beads for 1 h at 4°C with rotation and washed three times with lysis buffer.

Expression of amino-terminal fragments of PI3K_68D was performed in BL21(DH3) cells essentially as for the GST fusion proteins.

(iii) In vitro binding assays. Clarified extracts from flies and bacteria were incubated with immobilized GST or GST fusion proteins (20 μg) for 2 h at 4°C with rotation. Complexes bound to the beads were recovered by centrifugation, washed three times with lysis buffer, and heated to 95°C for 5 min in sodium dodecyl sulfate (SDS) sample buffer.

(iv) Immunoblotting. Extracts were resolved on SDS-polyacrylamide gels, transferred to nitrocellulose, and incubated with 9E10 to detect the Myc epitope. For analysis of wild-type and catalytically inactive PI3K_68D, blots were incubated with 9E10 mouse ascites (1/10,000; Developmental Studies Hybridoma Bank) and detected with horseradish peroxidase-linked anti-mouse immunoglobulin G (1/1,000; DAKO) by using ECL (Amersham). For analysis of complexes bound to GST fusion proteins, detection was with horseradish peroxidase-coupled anti-mouse IgG (1/10,000; Pierce) and the SuperSignal West Pico chemiluminescent substrate (Pierce).

(v) Assay of PI3K activity. PI3K assays were performed as described previously (40), using PI (Sigma) as a substrate, and resolved by thin-layer chromatography in chloroform–methanol–4.9 M ammonium hydroxide (50:39:11). The radioactivity was detected with a PhosphorImager (Molecular Dynamics).

Adult phenotypic analyses. Wings from female flies were dehydrated in ethanol and mounted in Euparal (Agar Scientific). Images were collected with a Leaf Microlumina color charge-coupled device camera (ISS, Greater Manchester, United Kingdom).

RESULTS

Analysis of class II PI3K function by ectopic expression. To identify the biological function of the class II PI3K in a multicellular organism, we expressed wild-type and mutated versions of *PI3K_68D* in different patterns during *Drosophila* imaginal disk development and looked for phenotypes in the adult cuticle. cDNAs for *PI3K_68D* were fused to an epitope tag and cloned into P-element expression vectors under the control of yeast Gal4 UASs (9).

Ectopic expression of the class I and class II PI3Ks generates distinct phenotypes. Ectopic expression of the class I PI3K, Dp110, has been shown to enhance organ size by increasing the size of cells without perturbing patterning (37, 72). To evaluate differences between the two classes of PI3Ks, the effects of their expression were directly compared by using a promoter that drives expression at high levels within the prospective wing blade. The wing is a flat structure, and hence

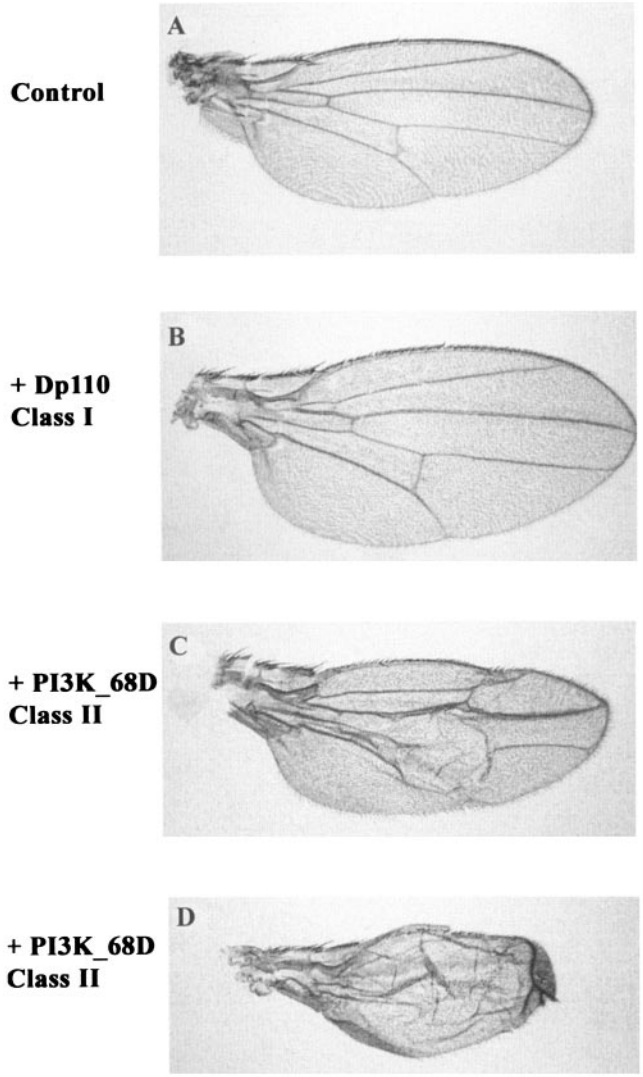

FIG. 1. Ectopic expression of the class I PI3K affects organ size, while ectopic expression of the class II PI3K affects patterning. Wings of a female control fly (Gal4-MS1096/+) (A) or of female flies expressing wild-type Dp110 (Gal4-MS1096/+; UAS-*WT-Dp110*/+) (B) or PI3K_68D (Gal4-MS1096/+; UAS-WT-*PI3K_68D*/+) (C and D) in the precursor to the wing blade are shown. Crosses were performed at 25°C (A, B, and D) or 18°C (C).

changes in size can be easily visualized. The two PI3Ks generated distinct phenotypes (Fig. 1), indicating that class I and class II PI3Ks target distinct pathways. Ectopic expression of the class I PI3K generated a larger wing, as has been previously described (37). In contrast, ectopic expression of the class II PI3K, *PI3K_68D*, generated very severe developmental defects. When larvae were reared at 18°C rather than at 25°C to induce weaker expression of *PI3K_68D*, the phenotypic effects obtained were less severe although variable. An example of a weak phenotypic effect is shown in Fig. 1C. Effects on the patterning of the wing veins were observed. In addition, many of the wings were blistered, presumably because the two surfaces of the wing blade failed to adhere properly. In contrast to ectopic expression of the class I PI3K, overgrowth of the wing never occurred with ectopic *PI3K_68D* expression.

While these phenotypes provided a dramatic illustration of the differences in signaling between the class I and class II PI3Ks, those generated by expression of *PI3K_68D* were too severe and variable to look for genetic interactions with other signaling components. We therefore also generated a version of *PI3K_68D* that was predicted to be inactive, in order to determine the effects of decreasing the level of class II PI3K signaling. This construct contained a mutation in an aspartate residue (D1457A) that lies within the activation loop of the PI3K catalytic domain and is predicted to contact a metal ion (70). The corresponding residue within protein kinases has been shown to be critical for catalytic activity.

The biochemical properties of these proteins were assessed following heat shock-induced expression in adult flies. The ectopically expressed PI3K was specifically immunoprecipitated from detergent lysates, using an antibody to the epitope tag, and assayed for lipid kinase activity. Figure 2A shows that expression of the wild-type, p210, PI3K (WT-*PI3K_68D*) was induced following heat shock and that this protein possessed PI3K activity. As anticipated, the construct containing the D1457A mutation lacked detectable PI3K activity when expressed at levels similar to those of the wild-type protein. We have designated this transgene KD-*PI3K_68D* (for kinase dead). Since the mutant PI3K is unable to generate the downstream lipid signal, it is predicted to have an inhibitory or dominant-negative effect on the function of the endogenous PI3K by competing with the endogenous PI3K for binding sites on interacting molecules. Hence, expression of the wild-type or catalytically inactive *PI3K_68D* constructs should increase or decrease the levels of the lipid signal, respectively.

Ectopic expression of wild-type or catalytically inactive versions of *PI3K_68D* have opposing effects on bristle number. In order to generate adult phenotypes, these *PI3K_68D* transgenic lines were crossed to a number of different enhancer-trap Gal4 lines to induce expression in specific developmental patterns within the larval imaginal disks. We have previously demonstrated that the endogenous enzyme is expressed and possesses lipid kinase activity at this developmental stage (40).

The expression domain of the *patched* (*ptc*) Gal4 line (29, 33) includes the scutellum, the shield-shaped structure at the base of the thorax. Expression of the WT- and KD-*PI3K_68D* transgenes with Gal4-*ptc* produced opposing and completely penetrant effects on the number of scutellar bristles (Fig. 2B to D). Enhancing the level of the lipid signal with the wild-type transgene resulted in a loss of bristles and was accompanied by a reduction in the size of the scutellum (Fig. 2C), while decreasing the level of the lipid signal with the KD transgene increased the number of the scutellar bristles (Fig. 2D). Hence, expression of catalytically active and inactive versions of *PI3K_68D* can elicit opposing phenotypic effects. Consistent with the effects of the class I PI3K on growth but not on patterning, expression of either wild-type or catalytically inactive versions of Dp110 with Gal4-*ptc* had essentially no effect on the number of scutellar bristles (results not shown).

Expression of the class II PI3K affects patterning of the wing imaginal disk. The Gal4 line 69B induces strong expression within the epidermis. Staining with a β-galactosidase reporter line and with an antibody to the Myc epitope, which

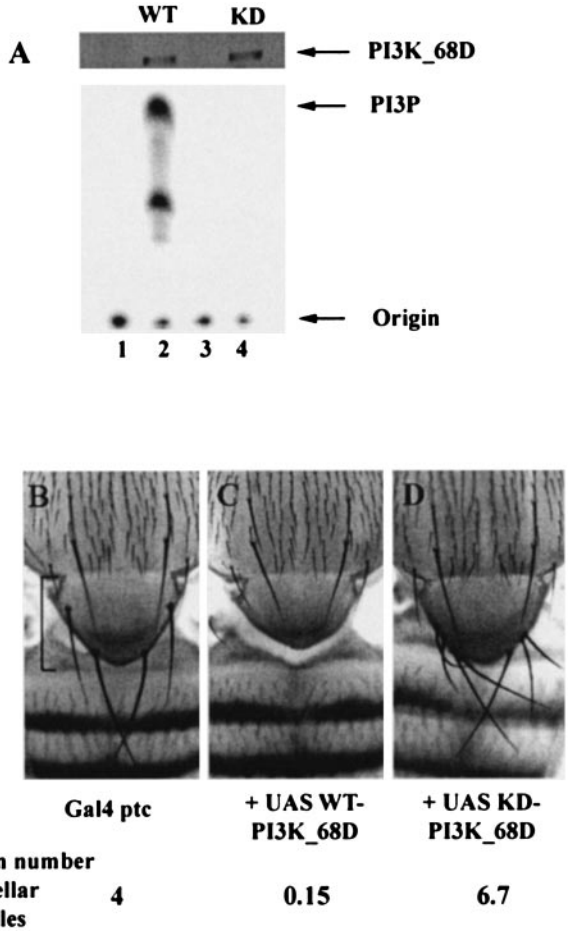

FIG. 2. Lipid-kinase-dependent phenotypic effects generated by expression of PI3K_68D. (A). Mutation of Asp1457 to Ala within the active site of PI3K_68D generates a catalytically inactive protein. Detergent lysates were prepared from adult flies expressing UAS-*PI3K_68D* constructs under the control of Gal4-heat shock promoters. The extracts were immunoprecipitated with an antibody to the Myc (9E10) epitope and assayed for PI3K activity with PI as a substrate. Equivalent levels of the two constructs were induced as shown by immunodetection with 9E10, but only the wild-type construct possessed PI3K activity (lane 2). Flies were of the following genotypes: lane 1, Gal4-hs/CyO; lane 2, Gal4-hs, UAS-*WT-PI3K_68D*/CyO; lane 3 Gal4-hs/TM3; lane 4, Gal4-hs, UAS-KD-*PI3K_68D*/TM3. Arrows mark the positions of the PI3K_68D protein at ~210 kDa, of PI3P, and of the origin. For each sample the equivalent of 0.5 or 2 female flies were used for the immunoblot (from extracts) and for the PI3K assay (from immunoprecipitations), respectively. Similar results were obtained in three separate experiments. (B to D) Ectopic expression of PI3K_68D affects the number of scutellar sensory bristles in a PI3K-dependent manner. Images of the thoraxes of adult female flies of genotypes Gal4-*ptc*/+ (B), Gal4-*ptc*/UAS-WT-*PI3K_68D* (C), and Gal4-*ptc*/+; UAS-KD-*PI3K_68D*/+ (D) are shown. The mean number of scutellar bristles for $n = 40$ nota is shown. The scutellum is indicated by a bracket. Normally, the four scutellar bristles point distally. In panel D some of these bristles remain curved upwards as in late stages of normal pupae, presumably because they fail to reorient themselves when the flies emerge. Crosses were performed at 25°C.

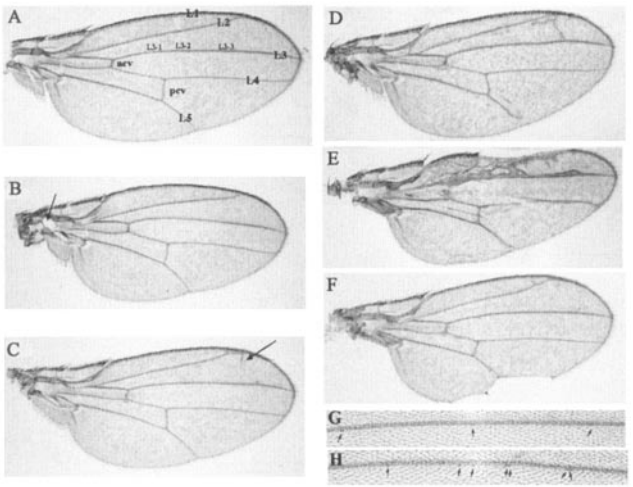

FIG. 3. Adult wing phenotypes generated by *PI3K_68D* transgenes with Gal4-69B. (A) A control wing expressing the Gal4-69B promoter alone generates an essentially wild-type wing characterized by five longitudinal veins (L1 to L5), two cross veins (anterior [acv] and posterior [pcv]), and a number of sensory elements, including the campaniform sensillae (A and G) on the distal portion of L3 (L3-1 to L3-3). (B) Expression of WT-*PI3K_68D* transgenes produced a small hole (arrow) within the proximal part of the first basal cell in the hinge region. This unusual phenotype was completely penetrant (at 25°C) and was observed with six different insertions. Frequently a hole was also observed in the haltere (not shown). (C to F) Most flies expressing KD-*PI3K_68D* under control of the Gal4-69B promoter produced mild ectopic wing vein material (C), but in a proportion of flies (D to F) a more severe range of patterning defects was observed. In panel D, a single ectopic cross vein (arrow) is produced between the distal end of L2 and vein L3. In panel E, multiple ectopic cross-veins are formed and there is a thickening of the longitudinal veins in the anterior region. Panels E and F show losses of portions of the wing margin. In panel E, the sensory bristles associated with the anterior wing margin occur at a higher density in the region proximal to the wing margin loss. (G and H) Section of L3 distal to the anterior cross vein which carries the L3-1 to L3-3 campaniform sensillae (see panel A). Flies expressing KD-*PI3K_68D* show supernumary campaniform sensillae (arrows) (H) compared to controls (Gal4-69B only) (G). The wings shown are from female flies of genotypes Gal4-69B/+ (A and G), WT-*PI3K_68D*/+; Gal4-69B/+ (B), and Gal4-69B/UAS-KD-*PI3K_68D* (C to F and H). Anterior is up; proximal is to the left.

identifies expression of the *PI3K* transgene, showed that Gal4-69B promoted expression within imaginal disks, such as the wing, haltere, and leg disks, and a restricted expression within the eye disks (reference 9 and data not shown). Within the wing disk, expression appeared to be highest in regions that give rise to the wing margin and within parts of the wing blade and hinge. We describe phenotypes generated with Gal4-69B and the *PI3K_68D* transgenes in the wing imaginal disk that affected the specification of the wing veins, wing margins, and sensory elements and the apposition of the wing surfaces.

The adult wing blade consists of two layers of ectodermal cells (dorsal and ventral) and is divided into regions of vein and intervein tissue by five longitudinal veins composed of more compact, highly pigmented cells (Fig. 3A). The veins provide structural support and form channels for neurons and trachea. The wing is further characterized by sensory organs such as the campaniform sensillae on the wing. These pattern elements, the sensory organs and veins as well as the large sensory bristles (macrochaetae) on the notum, occur in very precise locations (reviewed in reference 61). These are defined within the imaginal disks largely by the spatially restricted domains of expression of the proneural genes, *achaete* and *scute*, and the

TABLE 1. Catalytically inactive PI3K_68D wing phenotypes

Phenotype[a]	% Penetrance at[b]:	
	25°C	29°C
Ectopic cross vein L2-L3	5	25
Extensive ectopic wing venation	5	20
Wing margin loss	2	20

[a] The single cross vein L2-L3 phenotype is as shown in Fig. 3D.
[b] Flies were raised at the indicated temperatures. Values are for 100 flies at 25°C and for 41 flies at 29°C.

vein-promoting gene, *veinlet* (also known as *Rhomboid-1*). *veinlet* encodes a Golgi protein that regulates cleavage and hence the biological activity of the DER ligand, Spitz (36). In the third-instar wing disk, veinlet promotes the spatially restricted activation of mitogen-activated protein kinase (MAPK) by DER, and this directs wing cells into a vein specification pathway (64). During pupal development MAPK signaling is switched off in the prospective vein cells, allowing their differentiation (41), and the pattern is refined by the Notch and decapentaplegic signaling pathways, which restrict veins to their characteristic widths (18).

Ectopic expression of the WT-*PI3K_68D* with Gal4-69B principally affected structures derived from the wing imaginal disk, which gives rise to the wing blade, hinge, and notum (dorsal thorax), although effects on the legs and halteres were also observed. The hinge region, which joins the wing blade to the notum, was particularly sensitive to perturbations. WT-*PI3K_68D* expression resulted in a "held-out" wing phenotype that was accompanied by a small hole in the hinge intervein (Fig. 3B). Although many mutations produce a held-out wing phenotype, this is not accompanied by the small hole characteristic of *PI3K_68D* overexpression. Holes in the proximal part of the wing have been reported for overexpression of the *Rotund RacGap* and have been attributed to defects in adhesion (27). Higher levels of expression of WT-*PI3K_68D* additionally affected patterning of the wing blade and produced blisters, as with Gal4-MS1096 (Fig. 1), and occasionally resulted in complete loss of the wing blade itself. With high levels of WT-*PI3K_68D*, effects on viability were also observed, presumably because of expression within the embryo.

At 25°C, most flies expressing the catalytically inactive version of *PI3K_68D* with the Gal4-69B driver showed very minor amounts of additional wing vein material (Fig. 3C). However, a small proportion of the progeny displayed more severe phenotypes affecting the specification of wing veins and wing margins (Fig. 3D to F). The penetrance of these phenotypes was increased when the larvae were reared at 29°C, consistent with the established temperature sensitivity of the Gal4-UAS system (Table 1). This results in higher expression of transgenes with increased temperature. The effects on wing veins were most prominent in anterior regions of the wing and were frequently accompanied by a change in the wing shape resulting from a reduction in the size of anterior intervein regions (see, e.g., Fig. 3E). In some cases only a single ectopic cross vein formed between the distal end of L2, where it meets the anterior margin, and L3 (Fig. 3D); in others more extensive ectopic wing venation occurred (as in Fig. 3E). KD-*PI3K_68D* expression also affected wing margin formation, resulting in losses of portions of either the posterior wing margin (Fig. 3F) or the anterior wing margin with the concomitant loss of margin bristles (Fig. 3E).

Expression of KD-*PI3K_68D* also affected the external sense organs on the wing and thorax. The campaniform sensillae are dome-shaped sensory structures which are believed to sense strain on the wing cuticle (Fig. 3G). Expression of *KD-PI3K_68D* increased the number of the campaniform sensilla (Fig. 3H). As with the Gal4-*ptc* driver (Fig. 2D), Gal4-69B-mediated *KD-PI3K_68D* expression also generated supernumary bristles on the thorax (results not shown).

Specific mutations in components of the EGFR and Notch signaling pathways also affect wing veins, wing margins, and sensory structures, suggesting a link between these pathways and PI3K_68D signaling.

Class II PI3K interacts genetically with the EGFR and Notch signaling pathways. The dosage sensitivity of *KD-PI3K_68D* expressed with the Gal4-69B promoter allowed us to use this combination to look for interactions with genes that give similar mutant overexpression phenotypes. This approach can be used to identify signaling pathways in which the class II PI3Ks might be involved. The observed effects on the specification of wing veins and wing margins suggested links with the EGFR and Notch signaling pathways. The results in Fig. 4 demonstrate that wild-type and catalytically inactive *PI3K_68D* transgenes can interact genetically, and in an opposing fashion, with components of the EGFR signaling pathway in wing vein development. Furthermore, catalytically inactive PI3K_68D showed interactions with the Notch pathway.

Ellipse (*Egfr*^{ElpE1}) is a weak hypermorph of DER in which the first amino acid of the kinase domain ($A_{887}T$) is mutated (38). In transfected cells, this change results in ligand-independent autophosphorylation of the receptor. In the wing this mutation is associated with a weak extra-vein phenotype (6, 38). The ability of WT- and KD-*PI3K_68D* expression to modify *Egfr*^{ElpE1}-induced phenotypes was assessed. While a single copy of *Egfr*^{ElpE1} did not affect ectopic cross vein formation (Fig. 4D), when combined with the KD-*PI3K_68D* transgene it enhanced the penetrance of the formation of an ectopic L2-L3 cross vein from 5% (Fig. 4B) to 100% (Fig. 4E) of the progeny at 25°C. Conversely, one copy of the *Egfr*^{ElpE1} chromosome in combination with WT-*PI3K_68D* resulted in the loss of the anterior and posterior cross veins in a significant proportion of flies (Fig. 4F). These results show that the phenotype of a *DER* gain-of-function mutation can be enhanced by a catalytically inactive *PI3K_68D* and suppressed by a catalytically active *PI3K_68D*.

Argos is a secreted inhibitor of DER (reviewed in references 14 and 52). Ectopic expression of *argos* by using the Gal4-69B driver mimics loss-of-function mutations in *DER*. In the wing this results in the loss of wing veins, particularly L4 and the anterior cross vein, and a change in shape resulting from a loss of intervein tissue (Fig. 4G) (54). In addition, regions of L3 may be lost, and there is a prominent rough eye phenotype and a loss of the ocelli (simple eyes) and associated bristles on the head (reference 54 and data not shown). Coexpression of KD-*PI3K_68D* restored L4 to the wild-type pattern (Fig. 4H) without affecting the eye or ocelli phenotypes, while coexpression of the wild-type transgene enhanced the wing vein loss (Fig. 4I) with complete or partial loss of all veins except L5. Flies ex-

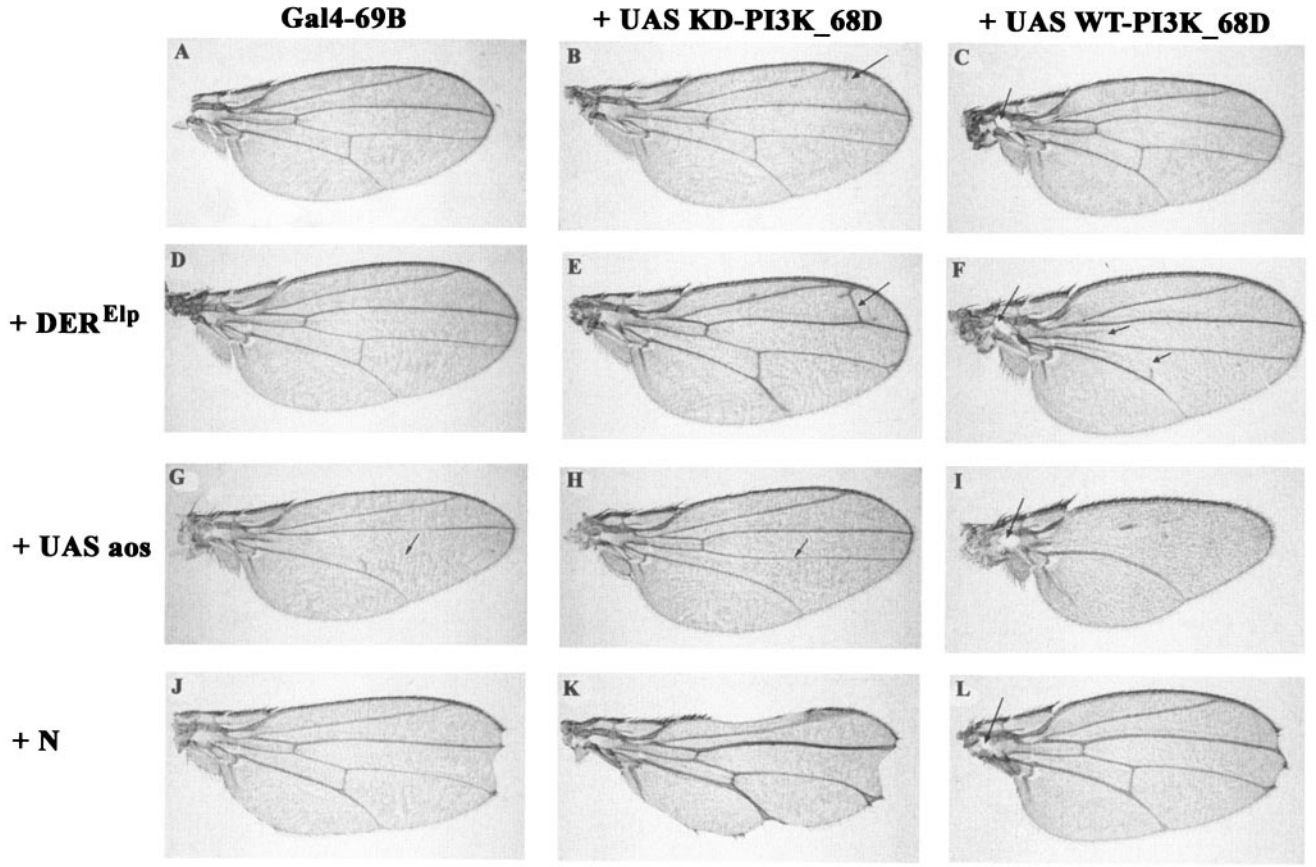

FIG. 4. Genetic interactions between *PI3K_68D* transgene phenotypes and components of the *Drosophila* EGFR and Notch signaling pathways. (A to C) At 25°C, expression of Gal4-69B alone produced an essentially wild-type wing (A), while expression of a KD-*PI3K_68D* transgene produced only mild ectopic wing vein material (B) and expression of a WT-*PI3K_68D* transgene produced a small hole within the hinge region (C). (D to F) One copy of an activated form of *DER* (Elp) alone had little effect on wing venation (D) but enhanced the formation of an ectopic cross vein in flies expressing UAS-KD-*PI3K_68D* from 5 to 100% at 25°C (for $n = 81$ flies and for two different KD-*PI3K_68D* insertions) (E) and the loss of the anterior (and partial loss of the posterior) cross vein in flies expressing UAS-WT-*PI3K_68D* (F). (G to I) Expression of *argos* (*aos*), a secreted inhibitor of DER, with Gal4-69B produced a narrower wing in which L4 and the anterior cross vein were missing (G). Coexpression of KD-*PI3K_68D* rescued L4 and the anterior cross vein but resulted in the loss of the posterior cross vein (H). Coexpression of WT-*PI3K_68D* enhanced the loss of wing veins (I). In addition to the loss of L4, the anterior cross vein, and the posterior cross vein, most of L3 and parts of L2 were deleted. Remnants of the latter veins, where present, occupied medial positions. (J to L) Loss-of-function mutations at the *Notch* locus (such as $N^{264\text{-}39}$) produce a characteristic notching of the wing margin at the anterior-posterior border (J). This was enhanced by expression of the UAS-KD-*PI3K_68D* transgene (K). In a small proportion of Notch flies, more severe wing notching is obtained. Similarly 2% of flies expressing catalytically inactive PI3K_68D at 25°C display a wing notching phenotype (Fig. 3E and F). Combinations of these more severe phenotypes presumably account for the small proportion of flies showing more severe interactions (not shown). Expression of WT-*PI3K-68D* did not enhance the loss-of-wing margin or the vein thickening of $N^{264\text{-}39}$ (L). Flies were raised at 25°C. The wings shown are from female flies of genotypes Gal4-69B/+ (A), Gal4-69B/UAS-KD-*PI3K_68D* (B), UAS-WT-*PI3K_68D*/+; Gal4-69B/+ (C), *Bc*, $Egfr^{ElpE1}$/+; Gal4-69B/+ (D), *Bc*, $Egfr^{ElpE1}$/+; Gal4-69B, UAS-KD-*PI3K_68D*/+ (E), UAS-WT-*PI3K_68D*/+; *Bc*, $Egfr^{ElpE1}$/+; Gal4-69B/+ (F), Gal4-69B/UAS-*aos* (G), Gal4-69B, UAS-KD-*PI3K_68D*/UAS-*aos* (H), UAS-WT-*PI3K_68D*/+; Gal4-69B/UAS-*aos* (I), $N^{264\text{-}39}$/+; Gal4-69B/+ (J), $N^{264\text{-}39}$/+; Gal4-69B, UAS-KD-*PI3K_68D*/+ (K), and $N^{264\text{-}39}$/UAS-WT-*PI3K_68D*; Gal4-69B/+ (L).

pressing *argos* and WT-*PI3K_68D* retained the prominent eye and ocelli phenotypes from *argos* expression and the hole in the hinge region generated by WT-*PI3K_68D* expression. Thus, targeted expression of WT-*PI3K_68D* enhanced and that of KD-*PI3K_68D* suppressed the wing vein loss generated by Argos, an inhibitor of the EGFR signaling pathway.

The wing margin forms at the dorsoventral compartment boundary following expression of transcription factors such as *vestigial* and *cut*, which are induced in response to Notch and wingless signaling. Consistent with this, specific loss-of-function mutations in *Notch* result in loss of parts of the wing margin (Fig. 4J). The loss of wing margin resulting from KD-*PI3K_68D* overexpression was enhanced by loss-of-function mutations in *Notch* such as $N^{264\text{-}39}$ (Fig. 4K) and *notchoid* (results not shown), demonstrating that PI3K_68D can also interact genetically with the Notch signaling pathway. The Notch-dependent loss of the wing margin was not enhanced by WT-*PI3K_68D* (Fig. 4L).

We were unable to identify specific mutations within the *PI3K_68D* gene among existing mutant stocks that mapped to this region. However, a deficiency which deleted one copy of the gene (Fig. 5), and hence presumably lowered the endogenous levels of the protein, interacted with the DER and Notch signaling pathway phenotypes in a manner similar to that for

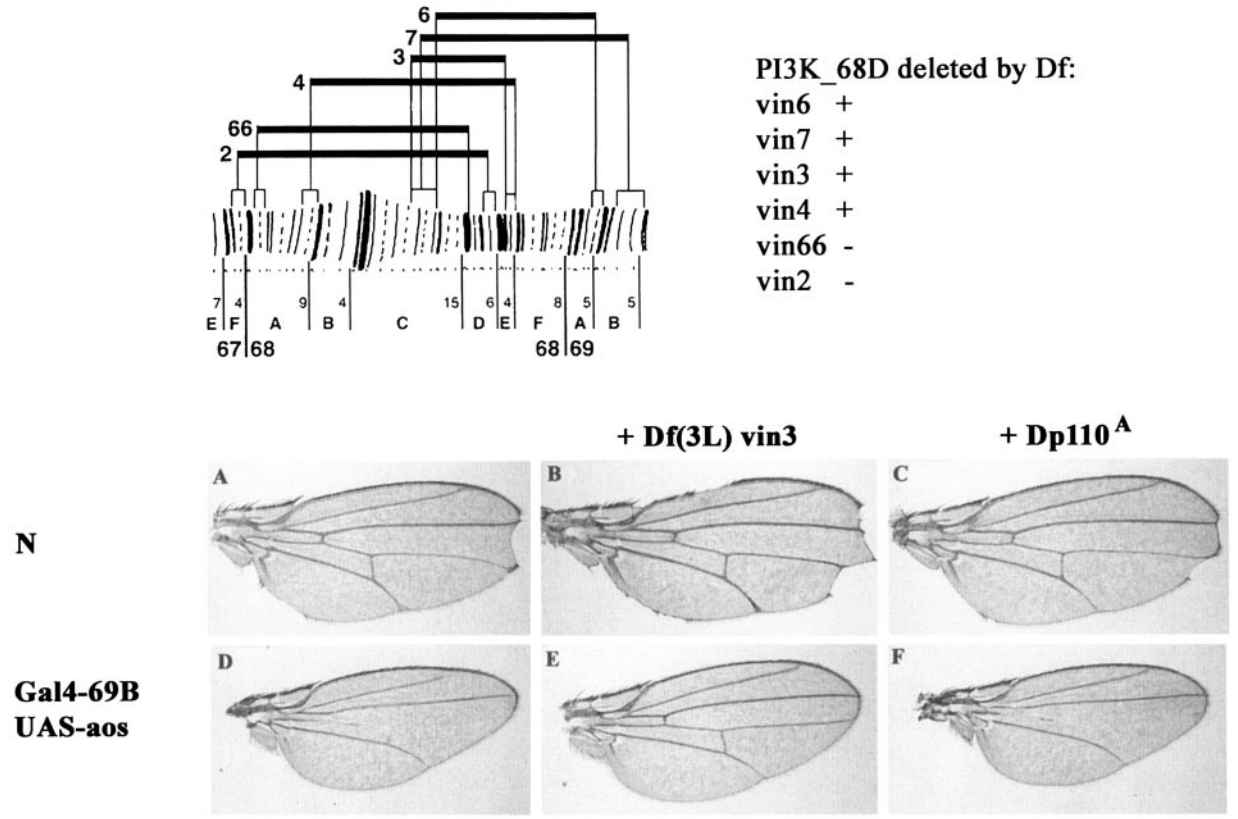

FIG. 5. Genetic interactions between *PI3K_68D* deficiencies and components of the *Drosophila* EGFR and Notch signaling pathways. (Top) Region of chromosome arm containing the *PI3K_68D* gene. Deficiency mapping by Southern hybridization showed that the *PI3K_68D* locus is uncovered by the deficiencies *Df*(*3L*)*vin3, Df*(*3L*)*vin4, Df*(*3L*)*vin6*, and *Df*(*3L*)*vin7* but excluded from *Df*(*3L*)*vin2* and *Df*(*3L*)*vin66*, placing it at ~68D6 to 68E3-4. This region probably contains five lethal complementation groups (31), including the genes *cyclin A* and *brachyenteron*. The chromosomal breakpoints of the *vin* deficiencies are from reference 1. (A to F) Notching of the wing margin by $N^{264\text{-}39}$ (A) is enhanced by a deficiency, *Df*(*3L*)*vin3*, which deletes the class II PI3K, *PI3K_68D* (B), but not by $Dp110^{A}$, which removes the class I PI3K, *PI3K_92E* (C). Similarly, the loss of the L4 wing vein on ectopic expression of *argos* (D) is rescued by *Df*(*3L*)*vin3* (E) but unaffected by $Dp110^{A}$ (F). Crosses were performed at 25°C. The wings shown are from female flies of genotypes $N^{264\text{-}39}$/+ (A), $N^{264\text{-}39}$/+; *Df*(*3L*)*vin3*/+ (B), $N^{264\text{-}39}$/+; $Dp110^{A}$/+ (C), Gal4-69B, UAS-*aos*/+ (D), Gal4-69B, UAS-*aos*/*Df*(*3L*)*vin3* (E), and Gal4-69B, UAS-*aos*/$Dp110^{A}$ (F).

the catalytically inactive *PI3K_68D* transgenes. Hence, *Df*(*3L*)*vin3* enhanced the wing margin loss associated with a *Notch* mutation and fully rescued the wing vein loss and shape change characteristic of *argo*s overexpression (Fig. 5). In contrast, a deletion at the cytological position 92E, termed $Dp110^{A}$, which specifically removes the class I PI3K, had no effect on the *Notch* and *argos* phenotypes. These results support our assumption that the catalytically inactive PI3K_68D acts in a dominant-negative manner and that the phenotypes it generates reflect a disruption of processes in which the endogenous *PI3K_68D* is involved. In addition, *Df*(*3L*)*vin3* suppressed the loss-of-bristle phenotype generated by Gal4-*ptc* WT-*PI3K_68D*, consistent with the deficiency decreasing the level of class II PI3K activity (results not shown).

PI3K_68D can bind the Drk adaptor protein in vitro. In order to investigate the mechanism by which *PI3K_68D* can interact genetically with the DER signaling pathway, we initially looked for a direct interaction between PI3K_68D and DER. Following coexpression of PI3K_68D and an activated version of DER in adult flies, we were unable to identify the Myc-tagged PI3K_68D in phosphotyrosine immunoprecipitates of activated DER (results not shown). Analysis of the PI3K_68D sequence had indicated a class II polyproline motif within a region of low complexity towards the N terminus of the molecule. This was predicted to act as a potential binding site for SH3 domains (40). In fact, this sequence, PPPLPPR, is identical to P1, one of the three proline-rich motifs within the C-terminal region of SOS, a guanine nucleotide exchange factor that activates Ras (50). The polyproline motifs within SOS bind the SH3 domains of Drk, the *Drosophila* homologue of mammalian Grb2. Drk is an adaptor protein that contains a phosphotyrosine binding SH2 domain flanked by two polyproline binding SH3 domains. Hence, Drk can link receptor tyrosine kinases with the activation of Ras and the MAPK pathway. A further sequence within PI3K_68D, RMQPTNP, located at amino acids 123 to 129 contains a basic residue N terminal to the polyproline core and hence conforms to the consensus for class I polyproline motifs (+xxPxxP).

We therefore investigated whether the Myc-tagged wild-type PI3K_68D expressed in adult flies could bind a GST-Drk fusion protein. As a control, an activated version of DER was also used. Both PI3K_68D and DER could associate with Drk (Fig. 6A). The interaction with DER is presumably via an interaction between the Drk SH2 domain and phosphotyrosine

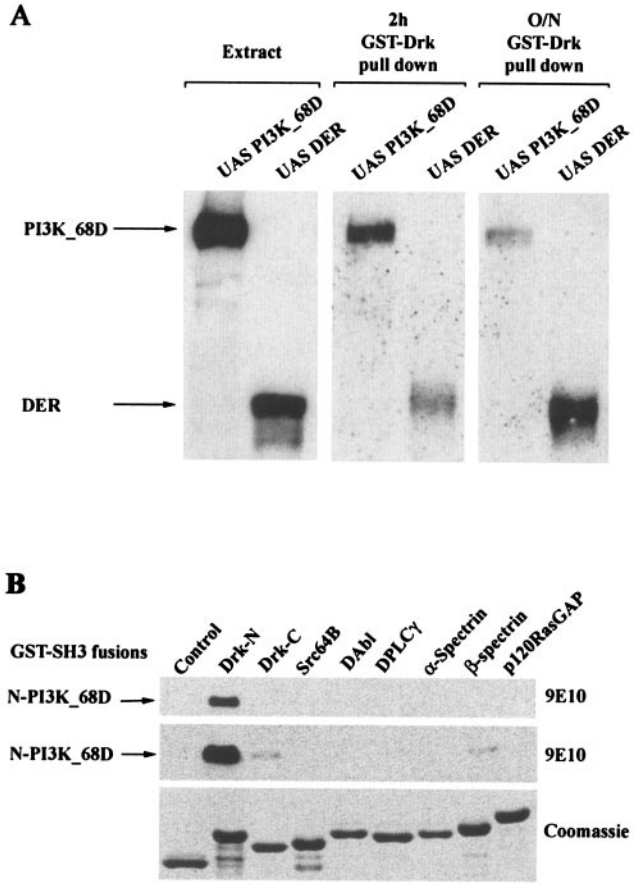

FIG. 6. PI3K_68D can associate with the adaptor protein Drk in vitro. (A) Extracts from 25 heat-shocked flies expressing Myc-tagged PI3K_68D or DER were incubated with GST-Drk (20 μg). Bound proteins equivalent to 1.5 flies (extracts) or 25 flies (pull-downs) were resolved by electrophoresis on an SDS–8% polyacrylamide gel, transferred to nitrocellulose, and detected with the 9E10 antibody. (B) Bacterial extracts expressing a Myc-tagged N-terminal fragment of PI3K_68D (20 μg) were incubated with GST alone (control) or with the different GST-SH3 fusion proteins shown (20 μg of each). An amount equivalent to 0.5 or 1% of each of the complexes bound to glutathione-Sepharose beads was resolved on an SDS–12% polyacrylamide gel, transferred to nitrocellulose, and detected with the 9E10 antibody. Upper and middle panels, proteins associated with 100 ng (upper) or 200 ng (middle) of GST-SH3 fusion proteins, respectively; lower panel, Coomassie blue-stained gel of the different fusion proteins (2 μg). Similar results were obtained in three separate experiments.

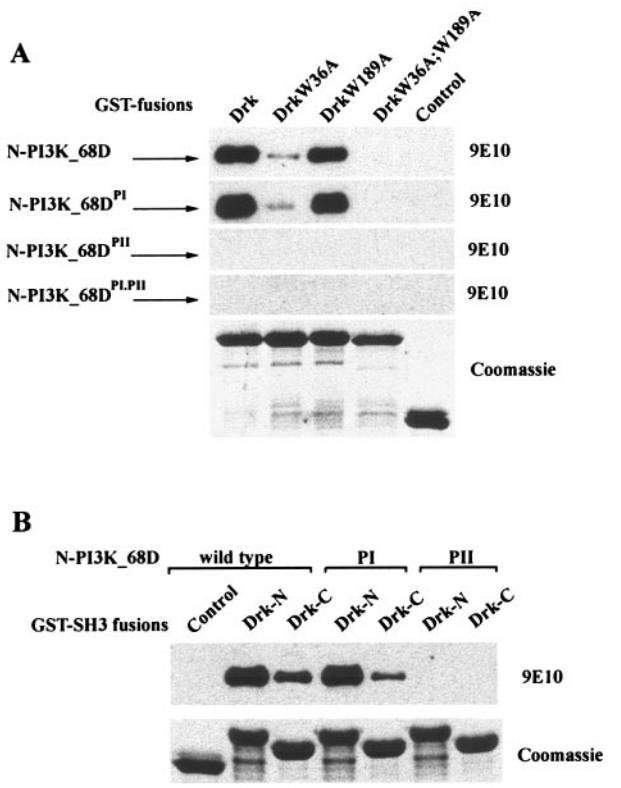

FIG. 7. A polyproline motif within PI3K_68D mediates binding to the SH3 domains of Drk. Bacterial extracts expressing Myc-tagged wild-type or mutant N-terminal fragments of PI3K_68D were incubated with the indicated GST-Drk fusion proteins (wild type or SH3 domain mutants) (20 μg). An amount equivalent to 0.5% of each of the complexes (100 ng of fusion protein) bound to glutathione-Sepharose beads was resolved on an SDS–12% polyacrylamide gel, transferred to nitrocellulose, and detected with the 9E10 antibody. The lower panel in each section shows a Coomassie blue-stained gel of the different fusion proteins (2.5 μg). Similar results were obtained in three separate experiments.

residues on DER. For PI3K_68D the interaction is predicted to be via the polyproline motif(s) in the N terminus of PI3K_68D and the SH3 domain(s) of Drk.

To investigate interactions mediated by these polyproline motifs in PI3K_68D, an N-terminal fragment containing the two polyproline motifs was generated and incubated with a panel of SH3 domains from a number of *Drosophila* signaling proteins. The N terminus of PI3K_68D showed a strong interaction only with the N-terminal SH3 domain of Drk. Weaker interactions were also observed with both the C-terminal SH3 domain of Drk and the SH3 domain of β_H-spectrin (Fig. 6B). No interactions were observed with the SH3 domains from a number of other signaling proteins. These included *Drosophila* phospholipase Cγ and Src64B. The mammalian homologues of these proteins have been reported to bind the EGFR, and hence it is possible that their SH3 domains may localize interacting molecules such that they can modify EGFR signaling. Similarly, no interaction was detected with *Drosophila* p120 RasGAP, a negative regulator of Ras; with DAbl, a non-receptor tyrosine kinase; or with α-spectrin, a cytoskeletal protein. Although the SH3 domains tested represented only a small proportion of those present in *Drosophila* (90 have been identified to date in the PFAM database [http://pfam.wustl.edu/cgi-bin/getdesc?name=SH3]), these results clearly show that there is specificity in the interaction between PI3K_68D and the SH3 domains of Drk. To investigate further the contributions made by the two SH3 domains of Drk in binding to the N terminus of PI3K_68D, we used wild-type Drk and Drk variants containing mutations in the highly conserved tryptophan residues (W36 in N-terminal SH3 and W189 in C-terminal SH3) (50). Binding of Drk to the N terminus of PI3K_68D was almost but not completely abolished by mutation of the N-terminal SH3 domain (Fig. 7A, top panel). In contrast, although binding was largely unaffected by mutation of the C-

TABLE 2. Effect of *drk* alleles on catalytically inactive PI3K_68D wing phenotypes

drk allele	% Penetrance of phenotype[a]	
	Single cross vein L2-L3	Multiple ectopic cross veins
–	22	7
drk^{10626} hypomorph	25	2
drk^{e0A} antimorph	3	0

[a] The single cross vein L2-L3 phenotype is as shown in Fig. 3D. Flies were raised at 30°C. Values are for 100 flies of each genotype.

terminal SH3 domain, a complete loss of binding occurred only when both domains were mutated. These results imply that the N-terminal SH3 domain is primarily responsible for the interaction of Drk with PI3K_68D.

In order to identify the region within PI3K_68D responsible for the interaction, the binding experiments were repeated with proteins containing mutations in the critical proline and arginine residues within either or both of the identified polyproline motifs (**R**MQ**P**TN**P** [PI] and P**PP**L**PP**R [PII]). Binding of Drk to the N-terminal fragment of PI3K_68D was largely unaffected by mutation of the first polyproline motif, PI (Fig. 7A, second panel), but the interaction was completely abolished by mutation of the second motif, PII (Fig. 7A, third panel). These results imply that a single polyproline motif within PI3K_68D can mediate the interaction with the adaptor protein Drk in vitro, primarily through binding to the N-terminal SH3 domain of Drk (Fig. 7A). To confirm these results, the wild-type and mutant (PI and PII) N-terminal PI3K_68D fragments were incubated with the isolated N- and C-terminal Drk SH3 domains. Consistent with the results obtained with the full-length Drk protein, binding of PI3K_68D to the N-terminal SH3 domain of Drk was significantly greater than that to the C-terminal SH3 domain and the interaction with both the N- and C-terminal SH3 domains was completely abolished when the PII polyproline motif was mutated (Fig. 7B). However, the results also implied that the C-terminal SH3 domain of Drk when expressed alone could bind to the PI sequence, as binding to the N-terminal fragment of PI3K_68D was consistently reduced when this PI sequence was mutated (Fig. 7B). Binding of the N-terminal fragment of PI3K_68D to the N-terminal SH3 domain was unaffected by mutation of the PI sequence (Fig. 7B), as was shown for the full-length Drk (Fig. 7A).

Genetic interactions between *drk* and a class II PI3K. In order to address the in vivo significance of the interaction observed between PI3K_68D and Drk, we looked for a genetic interaction between the *PI3K_68D* transgenes and the *drk* mutants. Since Drk acts downstream of the EGFR in wing vein formation (19a), *drk* loss-of-function alleles would be anticipated to suppress ectopic wing veins. While a single copy of either drk^{10626} or drk^{e0A} alone had no effect on wing vein formation, the drk^{e0A} allele suppressed the formation of ectopic veins generated by KD-*PI3K_68D* (Table 2). In the drk^{e0A} allele, His106 in the SH2 domain is mutated to Tyr (46). Since this mutant is probably unable to bind to tyrosine-phosphorylated proteins but may still bind to SOS, it most likely has a dominant-negative effect. Hence, it is likely to behave as a stronger mutant allele than the drk^{10626} hypomorphic allele, for which we were unable to observe an interaction. No interaction was observed between the *drk* mutant alleles and the WT-*PI3K_68D* transgene; this may be because the normal wing veins are less sensitive to perturbations than ectopic venation.

DISCUSSION

Ectopic expression of different classes of PI3Ks generates distinct phenotypes. We embarked on a phenotypic analysis of the class II *Drosophila PI3K* in order to identify developmental systems and signaling pathways in which this class of *PI3K* might be involved. In the absence of a mutation in the endogenous gene, we expressed *PI3K_68D* within *Drosophila* imaginal disks and looked at the effects on the adult cuticle. Class I and class II PI3Ks differ in their in vitro substrate specificity, and hence their presumed lipid signal, and in their domain structures, suggesting that they interact with different molecules. Consistent with these biochemical and structural properties, expression of these distinct classes of *PI3Ks* in vivo produced markedly different effects (Fig. 1).

Ectopic expression of the class I PI3K *(PI3K_92E*/Dp110) within imaginal disks generated effects on growth and final organ size without perturbing patterning. Moreover, this effect was observed in all adult structures derived from regions of Dp110 overexpression in the larval disks (37). In contrast, we found that PI3K_68D affected pattern elements, particularly the wing veins and margins (Fig. 3) and the sensory bristles on the notum and head. Notably, while patterning of the adult structures derived from the wing disk was affected by *PI3K_68D* expression with Gal4-69B, the eye appeared phenotypically normal. Similarly, the EGFR ligand, *vein*, affects wing veins but not the eye when expressed with Gal4-69B (reference 54 and data not shown). However, ectopic expression of a number of other molecules with this driver, such as the EGFR *DER*, *argos*, and *PI3K_92E*/Dp110, produced markedly rough or enlarged eyes in addition to the wing effects (reference 54 and unpublished observations). The lack of a detectable phenotype in the eye could be due to a threshold effect. Hence, the apparently ubiquitous effects of Dp110 expression may reflect a more linear response of growth and/or cell size to growth signals, while a threshold of signal may be required to trigger the changes in patterning observed with PI3K_68D.

Genetic interactions between PI3K_68D and the DER signaling pathway. The EGFR performs multiple functions in *Drosophila* development (reviewed in references 14 and 55). In imaginal disks, these functions include the specification of cell fate and the survival of postmitotic cells (21). Consequently, a variety of patterning defects are observed in the adult cuticle following an earlier reduction in DER function. These include the deletion of certain wing veins (principally L4 and the anterior cross vein), the duplication or elimination of specific sensory bristles, roughened compound eyes, and shrunken or missing ocelli (15). In the context of the wing imaginal disk, DER is locally activated within all vein primordia by *veinlet* and signals via the Ras-MAPK pathway to specify vein cell fate. Thus, activated (6) or overexpressed DER produces ectopic wing veins. Since expression of the catalytically inactive *PI3K_68D* generates a similar phenotype, we looked for genetic interactions between these molecules.

A hypermorphic mutation in *DER*, known as *Ellipse*, was able to enhance (Fig. 4E), and an antimorphic mutation in *drk* was able to suppress (Table 2), the penetrance of the ectopic cross vein phenotype produced by expressing the KD-*PI3K_68D* transgene. Similarly, this transgene suppressed the loss-of-veins phenotype induced by expression of the inhibitory *DER* ligand, *argos* (Fig. 4H), while the vein loss was enhanced by active *PI3K_68D* (Fig. 4I). These results suggest that PI3K_68D may act antagonistically to the Ras-MAPK pathway.

Examination of the sequence of PI3K_68D had previously identified a putative SH3 binding motif (40). In vitro binding studies demonstrated that this motif could interact with both SH3 domains of Drk (Fig. 6 and 7), an adaptor protein that links activated receptor tyrosine kinases such as DER to the Ras-MAPK signaling pathway. While the binding was mediated primarily by the N-terminal SH3 domain, the interaction was completely abolished only by the mutation of both N- and C-terminal SH3 domains. These results are consistent with the conservation in sequence between the class II polyproline motif in PI3K_68D and the P1 sequence in SOS, which interacts primarily but not exclusively with the N-terminal SH3 domain of Drk. In SOS the P1 sequence represents the highest-affinity site for Drk binding, but two further sequences may contribute to this effect.

The EGFR family in mammals has also been shown to recruit PI3Ks, although the mechanism involved is unclear. Indeed, one of the most frequent alterations in the EGFR that has been identified in human tumors (a deletion of exons 2 to 7, termed *EGFRvIII*, that results in ligand-independent receptor activation) may exert its transforming activity through a PI3K pathway (45). Recent results have indicated that the EGFR may signal through class II, in addition to class I, PI3Ks. First, only one of the four EGFR variants identified in mammals, ErbB3, contains the specific YXXM motifs recognized by the class I_A adaptor subunit, yet EGF stimulation of PI3K activity occurs in a number of cell types by an ErbB3-independent mechanism (62). Second, DER, which is equally similar structurally to the four mammalian EGFRs, lacks the YXXM motifs required for association with the class I PI3K. Third, overexpression of the class I_A PI3K, Dp110, does not affect wing venation (37) (Fig. 1). Recently the mammalian class II PI3Ks, PI3K-C2α and PI3K-C2β, have been identified in association with the EGFRs ErbB-1/ErbB-2 (2), implicating these mammalian class II PI3Ks in EGFR signaling. Within the N terminus of PI3K-C2β there is a cluster of three class II polyproline motifs analogous to the P1 to P3 sequences in SOS that bind Drk (73). Further analysis of the interaction between PI3K-C2β and the EGFR demonstrated that these sequences were required for the interaction and that they appeared to bind both the N- and C-terminal SH3 domains of the Drk homologue Grb2 (73). However, while PI3K-C2α has been reported to bind the activated EGFR, it lacks class II polyproline motifs. Furthermore, the third mammalian class II PI3K, PI3K-C2γ, also lacks these sequences. These structural differences indicate that the interaction with Grb2 cannot be essential for the function of all class II PI3Ks. The single *C. elegans* class II PI3K, however, contains multiple class II polyproline motifs within the N terminus which might interact with the Grb2 homologue, SEM-5. Hence, possession of a class II PI3K containing a class II polyproline motif appears to be conserved among multicellular organisms.

The Drk family of adaptor proteins has been shown to interact with a number of different molecules. In addition to interacting with the polyproline motifs in SOS primarily via the N-terminal SH3 domain (50), the C-terminal SH3 domain can bind the receptor substrate DOS via a novel motif (25). Both of these interactions are anticipated to activate the Ras pathway. In addition Drk/Grb2 family members have been reported to interact with a number of molecules that negatively regulate receptor tyrosine kinase signaling. Among these is c-Cbl, an E3 ubiquitin ligase that marks the EGFR for endocytosis and hence degradation (71). In worms, a tyrosine kinase, ARK-1, has also been shown to inhibit EGFR signaling, and it is dependent upon the Grb2 homologue SEM-5 for this function (32).

Our results suggest that PI3K_68D may negatively regulate Ras-MAPK signaling downstream of the EGFR. However, this cannot simply be due to PI3K_68D competing with SOS for Drk and hence reducing signaling through SOS to Ras and the MAPK pathway, because the wild-type and catalytically inactive transgenes exerted opposite effects on modified EGFR signaling (Fig. 4). Hence, the interaction with Drk may be a mechanism for localization that allows the catalytic activity of PI3K_68D to interfere with the Ras-MAPK pathway. The 3-phosphorylated lipids produced by PI3K_68D might induce downregulation of DER-mediated Ras-MAPK signaling via stimulation of, for example, an endocytic pathway. In this situation, expression of the catalytically inactive transgene could displace the endogenous PI3K_68D but be unable to promote endocytosis. This would enhance DER signaling at the plasma membrane and hence wing vein formation. In mammalian cells, receptor-mediated endocytosis has been shown to be important in the downregulation of the ErbB1 EGFR in response to its ligand EGF (reviewed in reference 56). Alternatively, these lipids could interfere with the activation of EGFR either directly or, for example, via the Notch signaling pathway. While receptor-mediated endocytosis downregulates EGF receptor signaling, this process appears to be required for ligand-stimulated Notch signaling (57; reviewed in reference 56).

Clearly, it will be important to mutate the polyproline motif in PI3K_68D and examine the effects in vivo.

Genetic interactions between PI3K_68D and the Notch signaling pathway. Notch has multiple roles in development, particularly in the control of cell fate (reviewed in references 5 and 10). In mammals, a number of diseases, including T-cell lymphoma and mammary gland tumors, have been linked to mutations in the human *Notch* genes (5). In *Drosophila*, loss-of-function phenotypes for *Notch* include an increase in the number of sensory bristles, a loss of wing margins, and thickened veins. All of these phenotypes were also observed on expression of catalytically inactive *PI3K_68D*. Furthermore, a deficiency which deletes *PI3K_68D* (Fig. 5) or the expression of KD-*PI3K_68D* (Fig. 4K) enhanced the wing notching phenotypes generated by specific *Notch* mutations (Fig. 4J). Although loss-of-function *Notch* mutations characteristically produce thicker veins, ectopic cross vein formation as observed for KD-*PI3K_68D* expression (Fig. 3D) has been induced through overexpression of an inhibitory version of Notch, the Notch

extracellular domain (51). Furthermore, activated versions of Notch (the *Abruptex* mutations) delete portions of the wing veins. Notch frequently acts antagonistically to the EGFR in cell fate specification (6, 19, 49; reviewed in reference 52). Hence, these phenotypes indicate that PI3K_68D may be acting downstream of, or parallel to, Notch in a pathway that negatively regulates EGFR signaling. Alternatively, PI3K_68D may influence Notch signaling through acting as a negative regulator of the EGFR pathway. There are several potential mechanisms for antagonism between these pathways. For example, Notch negatively regulates *veinlet* transcription in intervein cells and thus restricts veins to their characteristic widths. If PI3K_68D is a component of this pathway, expression of the catalytically inactive transgene may allow ectopic vein formation by relieving the inhibition on *veinlet* transcription in intervein regions. Veinlet, like PI3K_68D, potently affects EGFR signaling in the wing but not in the eye. Notch signaling can also upregulate *yan*, an Ets transcriptional repressor of multiple RTK signaling targets (53). In worms, receptor tyrosine kinase signaling can be inhibited through the Notch-dependent induction of LIP-1, a MAPK phosphatase (8). Conversely *ebi* and *strawberry notch*, two transcriptional targets of EGFR signaling in flies, can suppress Notch signaling (65).

Conclusions. The phenotypes that we have identified by ectopic expression demonstrate that class I and class II PI3Ks target distinct biological pathways. Whereas expression of the class I PI3K affects growth, our results show that expression of the class II PI3K perturbs patterning processes and may do so via effects on signaling by EGFR and the Notch receptor. Furthermore, the opposing phenotypes obtained with wild-type and catalytically inactive versions of PI3K_68D indicate a role for the class II PI3K-generated lipid signal in these processes. While it is necessary to be cautious in interpreting overexpression data, our results obtained by using deficiencies are consistent with the catalytically inactive PI3K_68D acting as a dominant-negative and disrupting processes in which the endogenous PI3K_68D is involved.

The adult cuticle phenotypes that we have identified from PI3K_68D expression can additionally be used for structure-function analyses of PI3K_68D and to screen for mutations, both within *PI3K_68D* itself and in genetically interacting molecules. We anticipate that these might include mutations in the EGFR and Notch signaling pathways. The identification of biological targets specific to class II PI3Ks will greatly facilitate the elucidation of specific roles for this class of PI3Ks in signaling pathways in both flies and mammals.

ACKNOWLEDGMENTS

This work was supported by grants from the BBSRC and from the Royal Society and by the Ludwig Institute. E.H. is supported by a grant from the Swiss National Science Foundation.

We thank Kathy Matthews and the Bloomington Stock Center, Mandy Simcox, and Christian Lehner for the fly stocks used in this study; the Developmental Studies Hybridoma Bank for the 9E10 supernatant; Tony Pawson for the GST-Drk, GST-Drk^{W36A}, and GST-Drk^{W189A} constructs; Simon Woodcock and David Hughes for the SH3 domain of p120 RasGAP; Brenda Catelani, Alan Entwhistle, Krishna Pitrola, and Heather Phillips for technical assistance; Juan Riesgo-Escovar and Christoph Hugentobler for help in generating transgenic lines; Jenny Higgs for advice on imaging thoraxes; Carmen Coelho, María Domínguez, Enrique Martín-Blanco, and members of the Hafen lab, past and present, for useful discussions; and David Hughes for constructive criticism of the manuscript.

REFERENCES

1. **Akam, M. E., D. B. Roberts, G. P. Richards, and M. Ashburner.** 1978. Drosophila: the genetics of two major larval proteins. Cell **13:**215–225.
2. **Arcaro, A., S. Volinia, M. J. Zvelebil, R. Stein, S. J. Watton, M. J. Layton, I. Gout, K. Ahmadi, J. Downward, and M. D. Waterfield.** 1998. Human phosphoinositide 3-kinase C2_β—the role of calcium and the C2 domain in enzyme activity. J. Biol. Chem. **273:**33082–33090.
3. **Arcaro, A., M. J. Zvelebil, C. Wallasch, A. Ullrich, M. D. Waterfield, and J. Domin.** 2000. Class II phosphoinositide 3-kinases are downstream targets of activated polypeptide growth factor receptors. Mol. Cell. Biol. **20:**3817–3830.
4. **Arcaro, A., U. K. Khanzada, B. Vanhaesebroeck, T. D. Tetley, M. D. Waterfield, and M. J. Seckl.** 2002. Two distinct phosphoinositide 3-kinases mediate polypeptide growth factor-stimulated PKB activation. EMBO J. **21:**5097–5108.
5. **Artavanis-Tsakonas, S., M. D. Rand, and R. J. Lake.** 1999. Notch signalling: cell fate control and signal integration in development. Science **284:**770–776.
6. **Baker, N. E., and G. M. Rubin.** 1992. Ellipse mutations in the Drosophila homologue of the EGF receptor affect pattern formation, cell division and cell death in eye imaginal discs. Dev. Biol. **150:**381–396.
7. **Basler, K., B. Christen, and E. Hafen.** 1991. Ligand-independent activation of the Sevenless receptor tyrosine kinase changes the fate of cells in the developing Drosophila eye. Cell **64:**1069–1081.
8. **Berset, T., E. F. Hoier, G. Battu, S. Canevascini, and A. Hajnal.** 2001. Notch inhibition of RAS signaling through MAP kinase phosphatase LIP-1 during C. elegans vulval development. Science **291:**1055–1058.
9. **Brand, A. H., and N. Perrimon.** 1993. Targetted gene expression as a means of altering cell fates and generating dominant phenotypes. Development **118:**401–415.
10. **Bray, S.** 1998. Notch signalling in Drosophila: three ways to use a pathway. Semin. Cell Dev. Biol. **9:**591–597.
11. **Brown, R., L. Ho, S. Weber-Hall, J. M. Shipley, and M. J. Fry.** 1997. Identification and cDNA cloning of a novel mammalian C2 domain-containing phosphoinositide 3-kinase, HsC2-PI3K. Biochem. Biophys. Res. Commun. **233:**537–544.
12. **Brown, R., J. Domin, A. Arcaro, M. D. Waterfield, and P. R. Shepherd.** 1999. Insulin activates the α isoform of class II phosphoinositide 3-kinase. J. Biol. Chem. **274:**14529–14532.
13. **Capdevila, J., and I. Guerrero.** 1994. Targetted expression of the signalling molecule decapentaplegic induces pattern duplications and growth alterations in Drosophila wings. EMBO J. **13:**4459–4468.
14. **Casci, T., and M. Freeman.** 1999. Control of EGF receptor signalling: lessons from fruitflies. Cancer Metast. Rev. **18:**181–201.
15. **Clifford, R. J., and T. Shübach.** 1989. Coordinately and differentially mutable activities of torpedo, the Drosophila melanogaster homologue of the vertebrate EGF receptor gene. Genetics **123:**771–787.
16. **Cohen, S. M.** 1993. Imaginal disc development, p. 747–842. *In* M. Bate and A. Martinez-Arias (ed.), The development of Drosophila melanogaster, vol. 2. Cold Spring Harbor Laboratory Press, Cold Spring Harbor, N.Y.
17. **Crosby, M. A., and E. M. Meyerowitz.** 1986. Lethal mutations flanking the 68C glue gene cluster on chromosome 3 of Drosophila melanogaster. Genetics **112:**785–802.
18. **de Celis, J. F., S. Bray, and A. Garcia-Bellido.** 1997. Notch signalling regulates Veinlet expression and establishes boundaries between veins and interveins in the Drosophila wing. Development **124:**1919–1928.
19. **Diaz-Benjumea, F. J., and A. Garcia-Bellido.** 1990. Behaviour of cells mutant for an EGF receptor homologue of Drosophila in genetic mosaics. Proc. R. Soc. London Biol. **242:**36–44.

19a. **Diaz-Benjumea, F. J., and E. Hafen.** 1994. The sevenless signalling cassette mediates Drosophila EGF receptor function during epidermal development. Development **120:**569–578.

20. **Domin, J., F. Pages, S. Volinia, S. E. Rittenhouse, M. J. Zvelebil, R. C. Stein, and M. D. Waterfield.** 1997. Cloning of a human phosphoinositide 3-kinase with a C2 domain that displays reduced sensitivity to the inhibitor wortmannin. Biochem. J. **326:**139–147.
21. **Domínguez, M., J. D. Wasserman, and M. Freeman.** 1998. Multiple functions of the EGF receptor in Drosophila eye development. Curr. Biol. **8:**1039–1048.
22. **Dove, S. P., F. T. Cooke, M. R. Douglas, L. G. Sayers, P. J. Parker, and R. H. Michell.** 1997. Osmotic stress activates phosphatidylinositol-3,5-bisphosphate synthesis. Nature **390:**187–192.
23. **Evan, G. I., G. K. Lewis, G. Ramsay, and G. M. Bishop.** 1985. Isolation of monoclonal antibodies specific for human c-*myc* proto-oncogene product. Mol. Cell. Biol. **5:**3610–3616.
24. **Feldmann, P., E. N. Eischer, S. J. Leevers, E. Hafen, and D. A. Hughes.** 1999. Control of growth and differentiation by Drosophila RasGAP, a homolog of p120 Ras-GTPase-activating protein. Mol. Cell. Biol. **19:**1928–1937.
25. **Feller, S. M., H. Wecklein, M. Lewitzky, E. Kibler, and T. Raabe.** 2002. SH3 domain-mediated binding of the Drk protein to Dos is an important step in signalling of Drosophila receptor tyrosine kinases. Mech. Dev. **116:**129–139.

26. **Guan, K. L., and J. E. Dixon.** 1991. Eukaryotic proteins expressed in *Escherichia coli*: an improved thrombin cleavage and purification procedure of fusion proteins with glutathione S-transferase. Anal. Biochem. **192:**262–267.
27. **Guichard, A., E. Bergeret, and R. Griffin-Shea.** 1997. Overexpression of Rn RacGAP in Drosophila melanogaster deregulates cytoskeletal organisation in cellular embryos and induces discrete imaginal phenotypes. Mech. Dev. **61:**49–62.
28. **Herman, P. K., and S. D. Emr.** 1990. Characterization of VPS34, a gene required for vacuolar protein sorting and vacuole segregation in *Saccharomyces cerevisiae*. Mol. Cell. Biol. **10:**6742–6754.
29. **Hinz, U., B. Giebel, and J. A. Campos-Ortega.** 1994. The basic-helix-loop-helix domain of Drosophila lethal of scute protein is sufficient for proneural function and activates neurogenic genes. Cell **76:**77–87.
30. **Ho, S. N., H. D. Hunt, R. M. Horton, J. K. Pullen, and L. R. Pease.** 1989. Site-directed mutagenesis by overlap extension using the polymerase chain reaction. Gene **77:**51–59.
31. **Hoogwerf, A. M., M. Akam, and D. Roberts.** 1988. A genetic analysis of the rose-gespleten region (68C8–69B5) of Drosophila melanogaster. Genetics **118:**665–670.
32. **Hopper, N. A., J. Lee, and P. W. Sternberg.** 2000. Ark-1 inhibits EGFR signalling in C. elegans. Mol. Cell **6:**65–75.
33. **Johnson, R. L., J. K. Grenier, and M. P. Scott.** 1995. Patched overexpression alters wing disc size and pattern: transcriptional and post-transcriptonal effects on Hedgehog targets. Development **121:**4161–4170.
34. **Kay, B. R., M. P. Williamson, and M. Sudol.** 2000. The importance of being proline: the interaction of proline-rich motifs in signaling proteins with their cognate domains. FASEB J. **14:**231–241.
35. **Kispert, A., B. G. Herrmann, M. Leptin, and R. Reuter.** 1994. Homologs of the mouse Brachyury gene are involved in the specification of posterior terminal structures in *Drosophila*, *Tribolium*, and *Locusta*. Genes Dev. **8:**2137–2150.
36. **Lee, J. R., S. Urban, C. F. Garvey, and M. Freeman.** 2001. Regulated intracellular ligand transport and proteolysis control EGF signal activation in *Drosophila*. Cell **107:**161–171.
37. **Leevers, S. J., D. Weinkove, L. K. MacDougall, E. Hafen, and M. D. Waterfield.** 1996. The *Drosophila* phosphoinositide 3-kinase Dp110 promotes cell growth. EMBO J. **15:**6584–6594.
38. **Lesokhin, A. M., S. Y. Yu, J. Katz, and N. E. Baker.** 1999. Several levels of EGF receptor signalling during photoreceptor specification in wild-type, Ellipse, and null mutant Drosophila. Dev. Biol. **205:**129–144.
39. **Linassier, C., L. K. MacDougall, J. Domin, and M. D. Waterfield.** 1997. Molecular cloning and biochemical characterisation of a Drosophila PI-specific phosphoinositide 3-kinase. Biochem. J. **321:**849–856.
40. **MacDougall, L. K., J. Domin, and M. D. Waterfield.** 1995. A family of phosphoinositide 3-kinases in Drosophila identifies a new mediator of intracellular signalling. Curr. Biol. **5:**1404–1415.
41. **Martín-Blanco, E., F. Roch, E. Noll, A. Baonza, J. B. Duffy, and N. Perrimon.** 1999. A temporal switch in DER signalling controls the specification and differentiation of veins and interveins in the Drosophila wing. Development **126:**5739–5747.
42. **Milan, M., F. J. Diaz-Benjumea, and S. M. Cohen.** 1998. Beadex encodes an LMO protein that regulates Apterous LIM-homeodomain activity in Drosophila wing development: a model for LMO oncogene function. Genes Dev. **12:**2912–2920.
43. **Misawa, H., M. Ohtsubo, N. Copeland, D. Gilbert, N. Jenkins, and A. Yoshimura.** 1998. Cloning and characterisation of a novel class II phosphoinositide 3-kinase containing a C2 domain. Biochem. Biophys. Res. Commun. **244:**531–539.
44. **Molz, L., Y. Chen, and L. T. Williams.** 1996. Cpk is a novel class of Drosophila PtdIns 3-kinase containing a C2 domain. J. Biol. Chem. **271:**13892–13899.
45. **Moscatello, D. K., M. Holgado-Madruga, D. R. Emlet, R. B. Montgomery, and A. J. Wong.** 1998. Constitutive activation of phosphatidylinositol 3-kinase by a naturally occurring mutant epidermal growth factor receptor. J. Biol. Chem. **273:**200–206.
46. **Olivier J.-P., T. Raabe, M. Henkemeyer, B. Dickson, G. Mbamalu, B. Margolis, J. Schlessinger, E. Hafen, and T. Pawson.** 1993. A Drosophila SH2-SH3 adaptor protein implicated in coupling the sevenless tyrosine kinase to an activator of Ras guanine nucleotide exchange, Sos. Cell **73:**179–191.
47. **Ono, F., T. Nakagawa, S. Saito, Y. Owada, H. Sakagami, K. Goto, M. Suzuki, S. Matsuno, and H. Kondo.** 1998. A novel class II phosphoinositide 3-kinase predominantly expressed in liver and its enhanced expression during liver regeneration. J. Biol. Chem. **273:**7731–7736.
48. **Ponting, C. P.** 1996. Novel domains in NADPH oxidase subunits, sorting nexins, and PtdIns 3-kinases: binding partners of SH3 domains? Protein Sci. **5:**2353–2357.
49. **Price, J. V., E. D. Savenye, D. Lum, and A. Breitkreutz.** 1997. Dominant enhancers of Egfr in Drosophila melanogaster: genetic links between the Notch and EGFR signalling pathways. Genetics **147:**1139–1153.
50. **Raabe, T., J. P. Olivier, B. Dickson, X. Liu, G. D. Gish, T. Pawson, and E. Hafen.** 1995. Biochemical and genetic analysis of the Drk SH2/SH3 adaptor protein of *Drosophila*. EMBO J. **14:**2509–2518.
51. **Rebay, I., R. G. Fehon, and S. Artavanis-Tsakonas.** 1993. Specific truncations of Drosophila Notch define dominant activated and dominant negative forms of the receptor. Cell **74:**319–329.
52. **Rebay, I.** 2002. Keeping the receptor tyrosine kinase signalling pathway in check: lessons from Drosophila. Dev. Biol. **251:**1–17.
53. **Rohrbaugh, M., E. Ramos, D. Nguyen, M. Price, Y. Wen, and Z. C. Lai.** 2002. Notch activation of yan expression is antagonized by RTK/pointed signaling in the Drosophila eye. Curr. Biol. **12:**576–581.
54. **Schnepp, B., T. Donaldon, G. Grumbling, S. Ostrowski, R. Schweitzer, B.-Z. Shilo, and A. Simcox.** 1998. EGF domain swap converts a Drosophila EGF receptor activator into an inhibitor. Genes Dev. **12:**908–913.
55. **Schweitzer, R., and B.-Z. Shilo.** 1997. A thousand and one roles for the Drosophila EGF receptor. Trends Genet. **13:**191–196.
56. **Seto, E. S., H. J. Bellen, and T. E. Lloyd.** 2002. When cell biology meets development: endocytic regulation of signalling pathways. Genes Dev. **16:**1314–1336.
57. **Seugnet, L., P. Simpson, and M. Haenlin.** 1997. Requirement for dynamin during Notch signaling in Drosophila neurogenesis. Dev. Biol. **192:**585–598.
58. **Shao, X., C. Li, I. Fernandez, X. Zhang, T. C. Südhof, and J. Rizo.** 1997. Synaptotagmin-syntaxin interaction: the C2 domain as a Ca^{2+}-dependent electrostatic switch. Neuron **18:**133–142.
59. **Simon, M. A., D. D. Bowtell, G. S. Dodson, T. R. Laverty, and G. M. Rubin.** 1991. Ras1 and a putative guanine nucleotide exchange factor perform crucial steps in signaling by the sevenless protein tyrosine kinase. Cell **67:**701–716.
60. **Simon, M. A., G. S. Dodson, and G. M. Rubin.** 1993. An SH3-SH2-SH3 protein is required for p21Ras1 activation and binds to sevenless and Sos proteins in vitro. Cell **73:**169–177.
61. **Simpson, P., R. Woehl, and K. Usui.** 1999. The development and evolution of bristle patterns in Diptera. Development **126:**1349–1364.
62. **Soltoff, S. P., S. A. Carraway, S. A. Prigent, W. G. Gullick, and L. C. Cantley.** 1994. ErbB3 is involved in activation of phosphatidylinositol 3-kinase by epidermal growth factor. Mol. Cell. Biol. **14:**3550–3558.
63. **Stephens, L. R., A. Eguinoa, H. Erdjument-Bromage, M. Lui, F. Cooke, J. Coadwell, A. S. Smrcka, M. Thelen, K. Cadwallader, P. Tempst, and P. T. Hawkins.** 1997. The Gβγ sensitivity of a PI3K is dependent upon a tightly associated adaptor, p101. Cell **89:**105–114.
64. **Sturtevant, M. A., M. Roark, and E. Bier.** 1993. The Drosophila Rhomboid gene mediates the localised formation of wing veins and interacts genetically with components of the EGF-R signalling pathway. Genes Dev. **7:**961–973.
65. **Tsuda, L., R. Nagaraj, S. Zipursky, and U. Banerjee.** 2002. An EGFR/Ebi/Sno pathway promotes delta expression by inactivating Su(H)/SMRTER repression during inductive Notch signaling. Cell **110:**625–637.
66. **Turner, S. J., J. Domin, M. D. Waterfield, S. G. Ward, and J. Westwick.** 1998. The CC chemokine monocyte chemotactic peptide-1 activates both the class I p85/p110 phosphatidylinositol 3-kinase and the class II PI3K-C2α. J. Biol. Chem. **273:**25987–25995.
67. **Vanhaesebroeck, B., S. J. Leevers, K. Ahmadi, J. Timms, R. Katso, P. C. Driscoll, R. Woscholski, P. J. Parker, and M. D. Waterfield.** 2001. Synthesis and function of 3-phosphorylated inositol lipids. Annu. Rev. Biochem. **70:**535–602.
68. **Virbasius, J. V., A. Guilherme, and M. P. Czech.** 1996. Mouse p170 is a novel phosphatidylinositol 3-kinase containing a C2 domain. J. Biol. Chem. **271:**13304–13307.
69. **Volinia, S., R. Dhand, B. Vanhaesebroeck, L. K. MacDougall, R. Stein, M. J. Zvelebil, J. Domin, C. Panaretou, and M. D. Waterfield.** 1995. A human phosphatidylinositol 3-kinase complex related to the yeast Vps34p-Vps15p protein sorting system. EMBO J. **14:**3339–3348.
70. **Walker, E. H., O. Perisic, C. Ried, L. Stephens, and R. L. Williams.** 1999. Structural insights into phosphoinositide 3-kinase signalling. Nature **402:**313–320.
71. **Waterman, H., M. Katz, C. Rubin, K. Shtiegman, S. Lavi, A. Elson, T. Jovin, and Y. Yarden.** 2002. A mutant EGF-receptor defective in ubiquitylation and endocytosis unveils a role for Grb2 in negative signalling. EMBO J. **21:**303–313.
72. **Weinkove, D., T. P. Neufeld, T. Twardzik, M. D. Waterfield, and S. J. Leevers.** 1999. Regulation of imaginal disc cell size, cell number and organ size by Drosophila class I_A phosphoinositide 3-kinase and its adaptor. Curr. Biol. **9:**1019–1029.
73. **Wheeler, M., and J. Domin.** 2001. Recruitment of the class II phosphoinositide 3-kinase C2β to the epidermal growth factor receptor: role of Grb2. Mol. Cell. Biol. **21:**6660–6667.
74. **Zhang, J., H. Banfic, F. Straforini, L. Tosi, S. Volinia, and S. Rittenhouse.** 1998. A type II phosphoinositide 3-kinase is stimulated via activated integrin in platelets. A source of phosphatidylinositol 3-phosphate. J. Biol. Chem. **273:**14081–14084.